ACS OMEGA

http://pubs.acs.org/journal/acsodf

Article

Synthesis, In Silico Studies, and In Vitro Anti-Inflammatory Activity of Novel Imidazole Derivatives Targeting p38 MAP Kinase

Archana Awasthi, Md Azizur Rahman,* and Mantripragada Bhagavan Raju

Cite This: *ACS Omega* 2023, 8, 17788−17799

Read Online

ACCESS | Metrics & More | Article Recommendations | Supporting Information

ABSTRACT: A series of eight novel *N*-substituted [4-(trifluoro methyl)-1*H*-imidazole-1-yl] amide derivatives (**AA1**−**AA8**) were synthesized, characterized, and evaluated for their in vitro p38 MAP kinase anti-inflammatory inhibitory activity. The synthesized compounds were obtained by coupling [4-(trifluoromethyl)-1*H*-imidazole-1-yl] acetic acid with 2-amino-*N*-(Substituted)-3-phenyl-propanamide derivatives utilizing 1-[bis(dimethylamino)-methylene]-1*H*-1,2,3-triazolo[4,5-*b*] pyridinium 3-oxide hexafluor-ophosphate as a coupling agent. Various spectroscopic methods established and confirmed their structures, specifically, ^{1}H NMR, ^{13}C NMR, Fourier transform infrared (FTIR), and mass spectrometry. In order to emphasize the binding site of the p38 MAP kinase protein and newly synthesized compounds, molecular docking studies were carried out. In the series, compound **AA6** had the highest docking score of 7.83 kcal/mol. The ADME studies were performed using web software. Studies revealed that all the synthesized compounds were orally active and showed good gastrointestinal absorption within the acceptable range. Lipinski's "rule of five" was used to determine drug-likeness. The synthesized compounds were screened for their anti-inflammatory activity by performing an albumin denaturation assay in which five compounds (**AA2**, **AA3**, **AA4**, **AA5**, and **AA6**) were found to exhibit substantial activity. Hence, these were further selected and proceeded for the evaluation of p38 MAP kinase inhibitory activity. The compound **AA6** possesses considerable p38 kinase inhibitory anti-inflammatory activity with an IC_{50} value of 403.57 ± 6.35 nM compared to the prototype drug adezmapimod (SB203580) with an IC_{50} value of 222.44 ± 5.98 nM. Some further structural modifications in compound **AA6** could contribute to the development of new p38 MAP kinase inhibitors with an improved IC_{50} value.

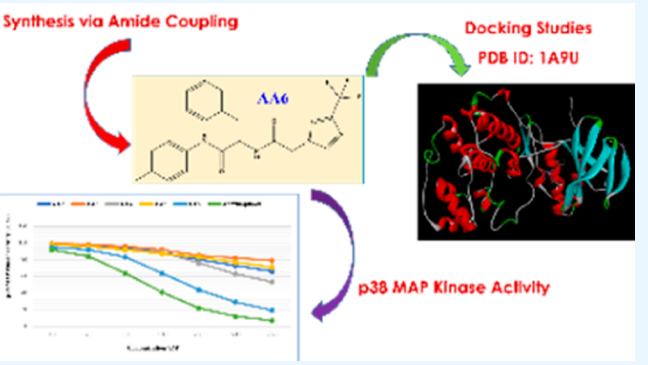

1. INTRODUCTION

Inflammation is a biological immune response that can be triggered by the host's response to a variety of factors such as pathogens, an infection caused by trauma or biological response, damaged cells, or toxic compounds, which can result in the production of reactive oxygen and nitrogen species, cytokinin release, and ultimately tissue damage. Chronic inflammation can develop from acute inflammation as a result of ongoing injury or personal circumstances (e.g., diabetes, obesity, use of corticosteroids, blood disorders, etc.). Inflammation leads to a variety of unpleasant symptoms and various diseases such as rheumatoid arthritis, inflammatory bowel disease, cardiovascular events, neurodegenerative conditions, cancer, COVID-19, and others.[1−7] Therefore, one of the main objectives in the field of drug discovery nowadays is the development of novel safe molecules with anti-inflammatory effects. Nonsteroidal anti-inflammatory drugs are commonly used as a medication to treat pain and inflammation.[8]

In terms of anti-inflammatory activity, drugs designed and developed to treat inflammation will target to inhibit either the inflammatory proteins (C-reactive protein, haptoglobin, alpha 1-acid glycoprotein, etc.) or enzymes (COX-2, LOX, PDE4, etc.) or inflammatory pathways (MAPK, NF-Kb, and JAK-STAT).[9]

Mitogen-activated protein kinases (MAPKs) are serine and threonine protein kinases that are found in eukaryotes and are involved in signal transduction pathways that regulate cell proliferation, differentiation, motility, and survival in mammals. The MAPK family includes three major members extracellular signal-regulated kinase, p38 MAPK, and c-Jun N-terminal kinase, which are involved in three different signaling cascades. Among them, p38 MAPK is considered a key role player in inflammation, a stress-induced kinase.[10] p38 MAPK family consists of four different isoforms, namely, p38 α, p38 β, p38 δ,

Received: January 30, 2023
Accepted: April 26, 2023
Published: May 12, 2023

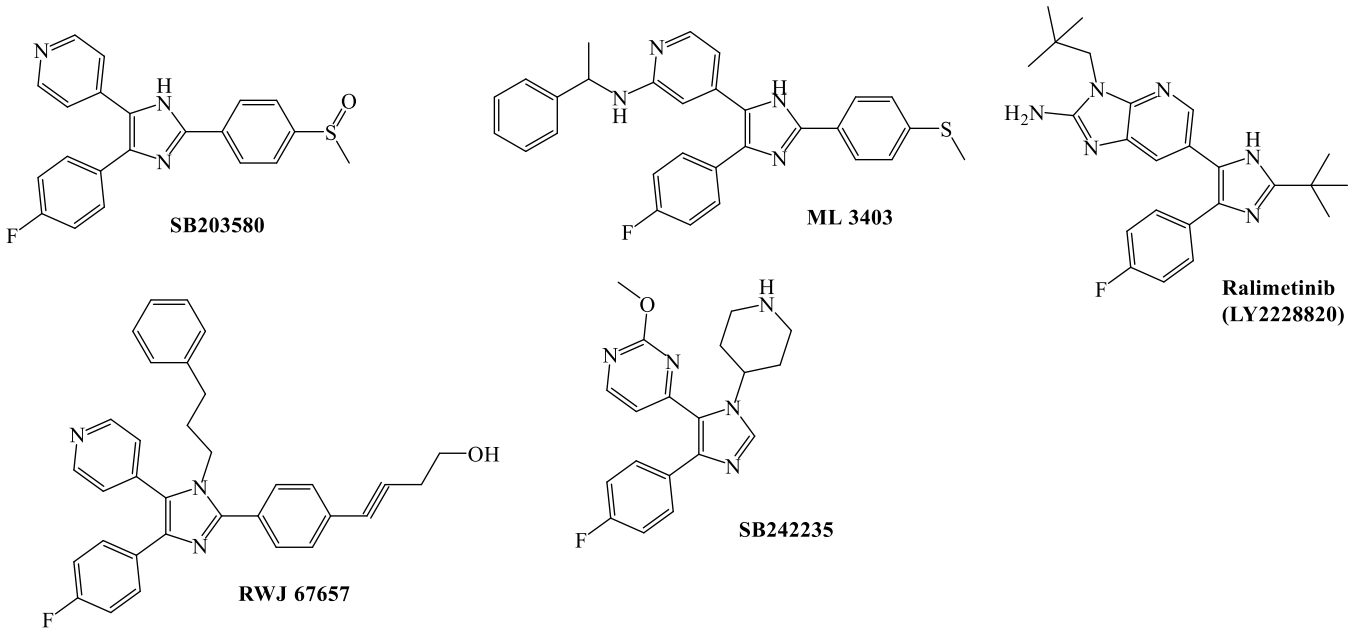

Figure 1. Imidazole-based p38 MAP kinase inhibitors.

and p38 γ.[11] All these forms are in different locations and show different cellular expressions. p38 α isoform is considered to be present in all cells and tissues. MAP kinases play a central role in regulating the production of pro-inflammatory cytokines including TNF-α, IL-1β, and IL-6. Various potent and selective p38 MAP kinase inhibitors are currently in phase II clinical studies for rheumatoid arthritis, psoriasis, inflammatory bowel diseases, neuropathic pain, cancer, depression, and cardiovascular diseases.[12]

SB203580 (adezmapimod) is a tri-substituted imidazole-based p38 MAP kinase inhibitor in the pyridinyl imidazole class that is widely used in the literature as an ATP-competitive ref 13. Several other novel imidazole derivatives, such as phenoxy pyrimidine, pyrazolo pyridines, benzimidazole, etc., have clinical significance as well, but only a few members of the pyridinyl imidazole class have progressed into clinical trials for the treatment of rheumatoid arthritis. None of the p38 MAP kinase inhibitors has been approved for market release. This could be due to a number of factors, including ineffectiveness, adverse effects, poor kinetics, or unspecific toxicity.[14] The reported imidazole-based p38 MAP kinase inhibitors are shown in Figure 1.

The aim of this research is to synthesize novel trifluoromethyl derivatives of imidazole via amide coupling of *t*-butyloxycarbonyl (Boc) protected phenylalanine with different amine derivatives. Amides are a vital class of organic molecules that have a wide range of applications as useful synthetic intermediates. They are formed by the direct condensation of carboxylic acids and amines, usually using a stoichiometric activating agent. Wide varieties of activators are used in medicinal chemistry as amide coupling via acid chloride, acid anhydride, activated ester, boron species, etc.[15] Amide bonds are fundamental in drug discovery because they are one of the basic linkages in all living systems.

Other approaches to amidation are thermal amidation, ester amidation, catalytic amidation, carbonylation, oxidative amidation, etc. Coupling reactions are performed either in solution or on a solid phase, depending on the nature of the amine. The solvent used in an amide coupling reaction is also very important. Dipolar aprotic solvents such as *N*-methyl-2-pyrrolidinone, *N*,*N*-dimethylformamide (DMF), CH_2Cl_2, and *N*,*N* dimethylacetamide are generally used.[16]

In this research, 2-[(*tert*-butoxycarbonyl) amino]-3-phenylpropanoic acid is coupled with various aromatic amine derivatives utilizing 1-[Bis(dimethylamino)methylene]-1*H*-1,2,3-triazolo[4,5-*b*] pyridinium 3-oxide hexafluorophosphate (HATU) as an activating/coupling agent and DMF as a dipolar aprotic solvent.

HATU is used when the coupling partners have a sensitive functional group. It provides faster couplings with less epimerization. It is also employed when the sterically hindered group is generally present. Due to its mild reaction conditions and usually high yields of amide product, this reagent has seen prevalent use as a coupling reagent for amide bond formation.[17]

2. RESULTS AND DISCUSSION

2.1. Chemistry. The synthesis of the *N*-substituted [4-(trifluoro methyl)-1*H*-imidazole-1-yl] amide derivatives (**AA1** to **AA8**) is a three-step reaction in which the second and third steps are based on coupling reactions. The detail of the reaction scheme is described in Figure 2. The structure of the final compounds is shown in Figure 3.

In the first step, 4-(trifluoromethyl)-1*H*-imidazole (**1**) was acetylated with ethyl bromoacetate (**2**) to afford the methyl [4-(trifluoromethyl)-1*H*-imidazole-1-yl] acetate (**3**) which on hydrolysis yield [4-(trifluoromethyl)-1*H*-imidazole-1-yl] acetic acid (**4**).

In the second step, commercially available (*t*-butoxycarbonyl)-L-phenylalanine (**5**) was treated with various amines (**A1** to **A8**) under a well-established method using HATU as the coupling agent in the presence of *N*,*N*-diisopropylethylamine (DIPEA) as a base to afford the {2-[(*t*-butoxycarbonyl) amino]-*N*-(substituted)}-3-phenylpropanamide derivatives (**KO-A1** to **KO-A8**) which were subsequently deprotected to yield 2-amino-*N*-(substituted)-3-phenyl propanamide derivatives (**KO-A1-D** to **KO-A8-D**).[18]

https://doi.org/10.1021/acsomega.3c00605
ACS Omega 2023, 8, 17788−17799

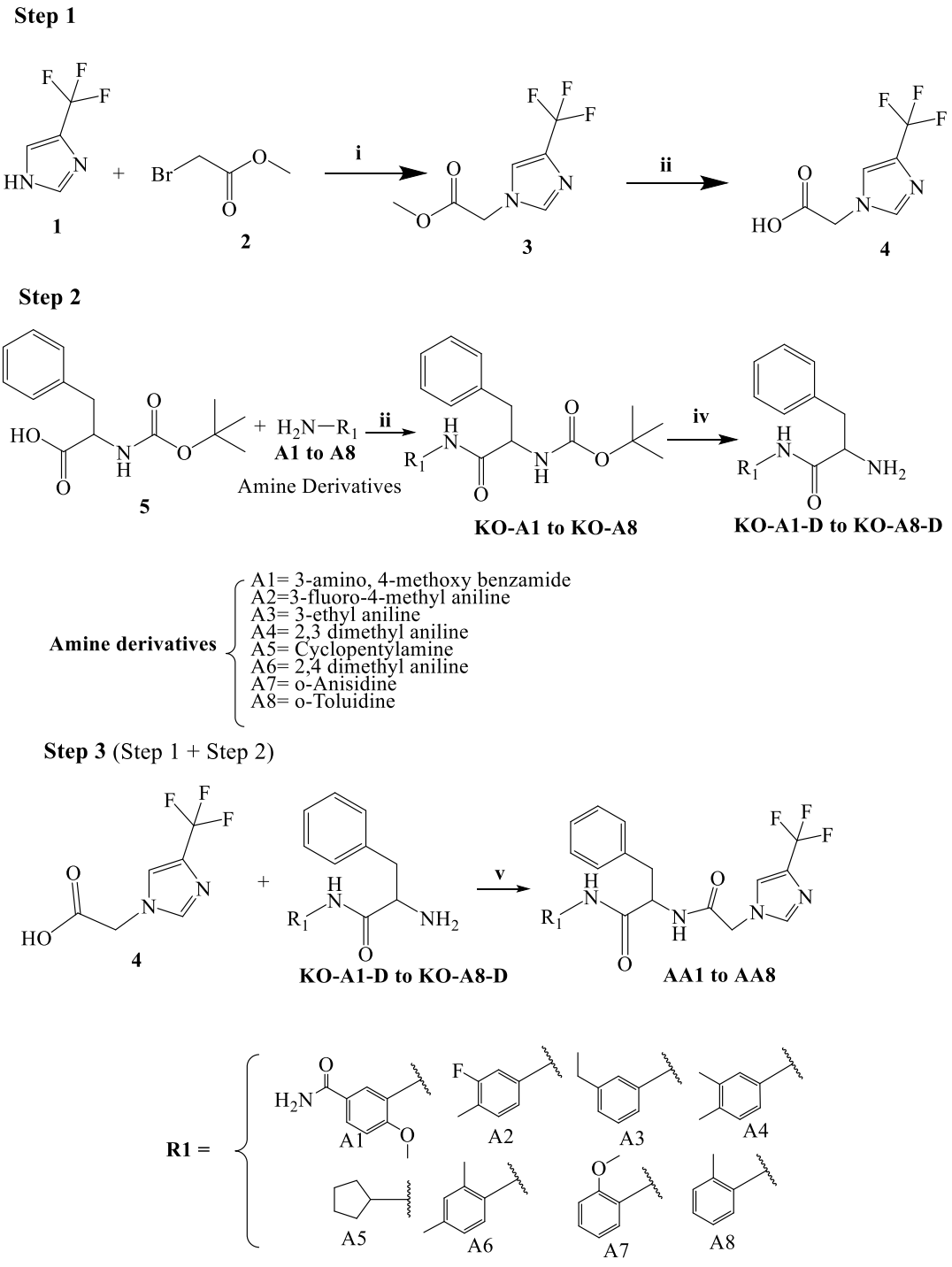

Figure 2. Reaction scheme showing the synthetic pathway of the *N*-substituted [4-(trifluoro methyl)-1*H*-imidazole-1-yl] amide derivative (**AA1**−**AA8**).

In step three, [4-(trifluoromethyl)-1*H*-imidazole-1-yl] acetic acid (**4**) from step 1 was coupled with KO-A1-D to KO-A8-D from step 2 using HATU to get the title compounds **AA1**−**AA8**. All the compounds were identified by spectral data like ^{1}H-NMR, ^{13}C NMR, Fourier transform infrared (FTIR), and mass spectrometry (MS).

The position of the proton (in the alphabet) is mentioned in Figure 4. There were two singlet amide peaks (a and c) between 7.5 ppm and 10 ppm chemical shift in ^{1}H NMR. The −CH_2 protons (d) attached to the imidazole ring exhibited a peak between 4.73 and 4.76 ppm. The two aliphatic hydrogens (g and h) of phenylalanine are in a different environment and hence display two distinct peaks at the range between 2.87−2.96 and 3.05−3.93 ppm, respectively. The most crucial linkage that justifies the production of the final compound is the aliphatic −CH proton (b), which is linked by two amide groups on both sides in the range of 4.48 and 4.90 ppm. In compounds AA1 and AA7, the chemical shift value shifted toward the downfield at 3.85 and 3.80 ppm, respectively, displaying a singlet peak as three protons are attached to oxygen. ^{13}C NMR spectra exhibited a peak between 54 and 56 ppm of chemical shift for all compounds showing the presence

https://doi.org/10.1021/acsomega.3c00605
ACS Omega 2023, 8, 17788−17799

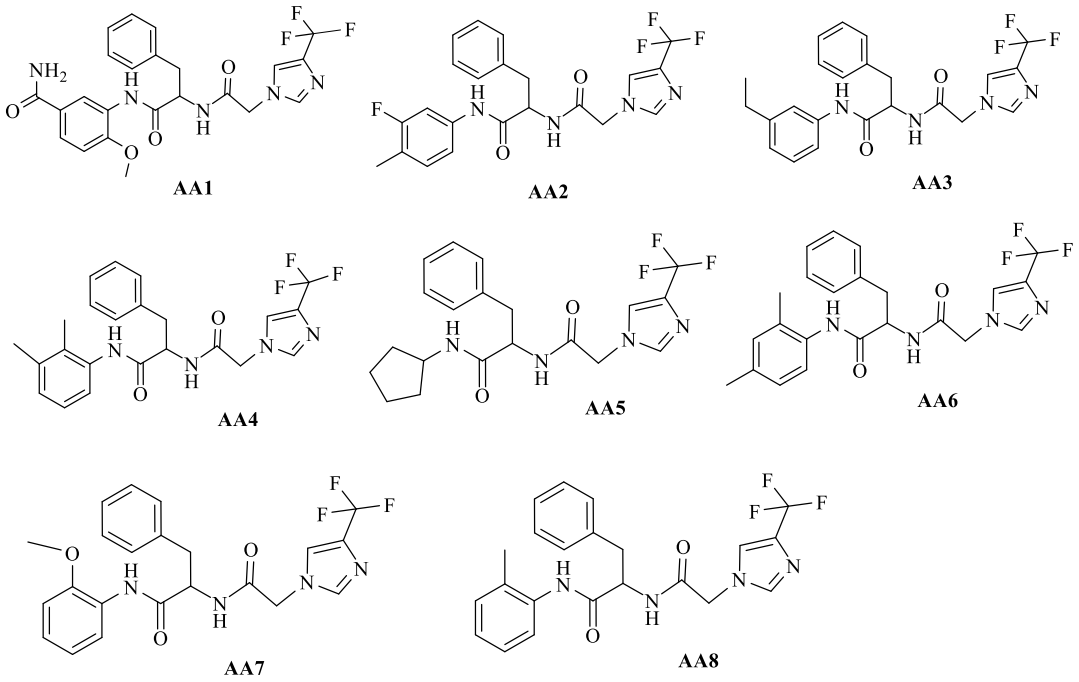

Figure 3. Structure of final synthesized compounds *N*-substituted [4-(trifluoro methyl)-1*H*-imidazole-1-yl] amide derivative (**AA1−AA8**).

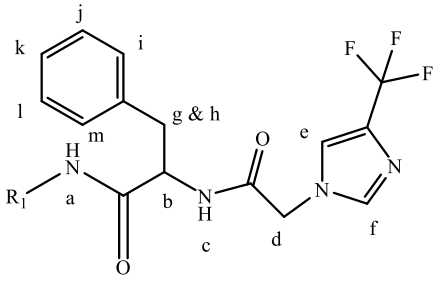

Figure 4. Position of protons (a−m).

of carbon which is linked by two amide groups on both sides. Methylene carbon is linked to the benzene and imidazole rings exhibiting a peak at 49 and 38 ppm, respectively. Carbon attached to three fluorine groups exhibited a peak near 121 ppm for all the compounds. In compounds, AA5 and AA8, two sharp peaks of DMF solvent were observed in ^{1}H NMR (2.72 and 2.88 ppm) and ^{13}C NMR (36.25 and 31.23 ppm). The FTIR spectrum of −NH stretching of amide showings an absorption band between 3265 and 3291 cm^{-1} and carbonyl group stretching is assigned for a peak between 1640 and 1651 cm^{-1}. All compounds (AA1−AA8) exhibited the corresponding M^{+1} peaks conforming to respective molecular formulas. All the spectral data results suggested AA1 to AA8 was successfully synthesized. The ^{1}H NMR, ^{13}C NMR, FTIR, and MS spectra of final compounds (AA1−AA8) and ^{1}H NMR spectra of all the intermediate compounds (KO-A1 to KO-A8, KO-A1-D to KO-A8-D, code 3, and code 4) were recorded in DMSO-d_6 and the peak assignment has been mentioned in the Characterization section and Supporting Information file.

2.2. In Vitro Anti-Inflammatory Activity. *2.2.1. Albumin Denaturation Inhibitory Activity.* Albumin denaturation inhibitory activity is one of the most commonly used assays for the preliminary evaluation of the anti-inflammatory activity of various compounds. The synthesized compounds AA1−AA8 were screened for anti-inflammatory activity by the inhibition of the albumin denaturation technique in four different concentrations such as 50, 100, 200, and 300 μg/mL

Table 1. Albumin Denaturation Inhibitory Activity of Test Samples

compounds	% inhibition of protein denaturation (mean ± SD)			
	Conc @ 50 μg/mL	Conc @ 100 μg/mL	Conc @ 200 μg/mL	Conc @ 300 μg/mL
AA1	19.25 ± 1.22	22.12 ± 1.88	34.22 ± 2.01	49.13 ± 3.25
AA2	18.23 ± 1.02	25.12 ± 1.86	36.28 ± 2.34	51.42 ± 3.45
AA3	19.65 ± 1.24	31.24 ± 2.01	45.21 ± 2.96	63.29 ± 3.25
AA4	25.36 ± 1.63	41.27 ± 2.34	59.22 ± 3.48	71.35 ± 3.95
AA5	22.14 ± 1.34	37.49 ± 2.65	48.23 ± 2.98	57.32 ± 3.46
AA6	39.55 ± 1.96	76.21 ± 3.54	87.69 ± 4.08	93.26 ± 4.66
AA7	21.25 ± 1.25	23.12 ± 1.76	32.22 ± 2.11	50.13 ± 3.37
AA8	20.23 ± 1.11	22.12 ± 1.72	38.28 ± 2.21	51.63 ± 3.22
diclofenac		82.53 ± 3.25		
control	8.47 ± 0.04			
negative control (DMSO @ 0.1%)	8.69 ± 0.03			

https://doi.org/10.1021/acsomega.3c00605
ACS Omega 2023, 8, 17788−17799

and showed anti-inflammatory activity in a dose-depending manner as listed in Table 1.

The IC_{50} values are shown in Figure 5. The synthesized compounds have IC_{50} values in the μg/mL range, varying from

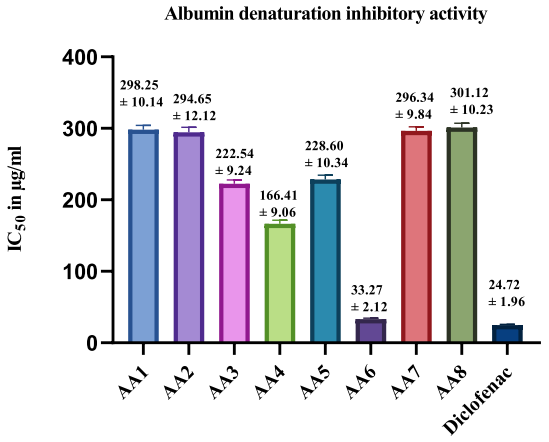

Figure 5. IC_{50} of Albumin denaturation inhibitory activity in μg/mL.

33.27 ± 2.12 to 301.12 ± 10.23 μg/mL compared to that of standard diclofenac (IC_{50} = 24.72 ± 1.96 μg/mL).

2.2.2. p38 MAP Kinase Anti-Inflammatory Inhibitory Activity. Among the synthesized derivatives, five compounds (AA2, AA3, AA4, AA5, and AA6) were found to exhibit substantial activity in the protein denaturation assay; hence, these compounds were further selected and proceeded for p38 MAP kinase inhibitory activity.

The p38 MAP kinase inhibitory activity of selected compounds is described in Table 2 and Figure 6. The effectiveness of the p38 kinase inhibitory activity was estimated with serial dilutions ranging from 10 to 1000 nM. It was observed that the p38 kinase inhibitory activity increases with the increase in concentration for all selected compounds. IC_{50} values of the p38 kinase enzyme inhibition are summarized in Figure 7. It has been observed that the compound contains dimethyl substitution at the second and fourth positions as AA6 (IC_{50} value of 403.57 ± 6.35 nM) exhibits considerable activity compared to the prototype drug adezmapimod (IC_{50} value 222.44 ± 5.98 nM), which infers that AA6 can contribute toward p38 MAP kinase activity.

2.3. Docking Analysis of p38 MAP Kinase Inhibitors. The docking study was performed to investigate the binding affinity of the novel *N*-substituted [4-(trifluoro methyl)-1*H*-imidazole-1-yl] amide derivative to the binding site of the p38 α MAP kinase protein. The docking scores of eight newly synthesized compounds (AA1 to AA8) and prototype drug SB203580 are shown in Table 3. Here, we describe the docking analysis of the three most potent compounds (AA4, AA6, and AA8) based on the docking score. All three potent compounds were found to include one or two methyl groups in their structures. AA6 showed the highest dock score of −7.83 kcal/mol followed by AA4 and AA8 with dock scores of −7.60 and −7.55 kcal/mol, respectively (AA6 > AA4 > AA8). Among them, the compounds with two methyl groups in their structures (AA6 and AA4) showed more binding interaction with receptors in comparison to compounds with one methyl group (AA8). All the molecules displayed similar molecular interactions with the active site of p38 MAP kinase and showed hydrogen bond interaction with amino acid residue Asp 168, Lys 53, and Tyr 35.

Hydrophobic interaction in form of the π-anion was observed between molecules and amino residues Glu 71. Amino acid residues Val 38, Val 39, Leu 74, Leu 75, Ile 84, and Ala 172 showed an hydrophobic interaction with docked molecules. Figure 8 depicts dock positions and molecular interactions of SB203580, while Figure 9 depicts that of the three most effective molecules AA8, AA6, and AA4 (AA6 > AA4 > AA8).

2.4. ADME Studies. Numerous techniques have been developed to quantify the drug-likeness of bioactive compounds based on topological descriptors of molecular structure or other features such as molecular weight, water solubility, cLogP, etc. Table 4 enlists the molecular characteristics of compounds (AA1−AA8). In this study, it was found that all the synthesized compounds (AA1−AA8) were orally active drugs based on Lipinski's rule of five, polar surface area (<140 $Å^2$), rotatable bonds (<10), lipophilicity (recommended range of −2.0 to 6.5), and the BOILED-egg or Ergan's egg approach. The graph indicated that all the compounds showed good gastrointestinal absorption (GIA) within the acceptable range (WLOGP ≤ 5.88 and TPSA ≤ 131.6), while one compound, AA6, is absorbed by the brain also. The blue dot indicates molecules predicted to be effluated from CNS by *p*-glycoprotein as in Table 5 and Figure 10.

3. CONCLUSIONS

In summary, various *N*-substituted [4-(trifluoromethyl)-1*H*-imidazole-1-yl] amide derivatives were synthesized to develop improved p38α MAP kinase inhibitors having significant anti-inflammatory activity. The compound AA6 emerged as the most potent compound in the series and shows considerable p38α MAP kinase inhibitory activity. Furthermore, the molecular docking study of compound AA6 demonstrated favorable orientation within the active binding site of p38α MAP kinase with the docking score comparable to that of the

Table 2. Effect of Selected Compounds on p38 MAP Kinase Activity

	p38 MAP kinase activity (in %) (mean ± SD)					
concentration (nM)	AA2	AA3	AA4	AA5	AA6	adezmapimod (SB203580)
10	99.23 ± 3.25	99.21 ± 4.17	98.32 ± 3.12	98.15 ± 3.14	95.07 ± 3.48	92.36 ± 4.15
25	97.24 ± 2.96	98.04 ± 2.56	96.33 ± 2.96	96.02 ± 2.86	92.18 ± 4.26	84.11 ± 3.25
50	94.15 ± 3.18	96.35 ± 2.94	92.14 ± 4.15	92.14 ± 3.42	83.52 ± 2.36	64.56 ± 2.96
100	89.21 ± 4.12	92.34 ± 3.21	89.93 ± 3.08	87.34 ± 3.55	64.01 ± 3.24	41.36 ± 3.48
250	80.45 ± 3.24	85.38 ± 3.48	76.21 ± 2.96	83.04 ± 3.75	44.35 ± 3.75	22.01 ± 4.25
500	73.12 ± 2.18	82.04 ± 3.12	63.01 ± 3.23	77.34 ± 3.28	29.75 ± 4.12	12.03 ± 3.75
750	66.35 ± 3.12	79.36 ± 2.01	53.17 ± 3.12	71.06 ± 4.21	19.52 ± 2.36	7.12 ± 2.96
1000	63.45 ± 3.32	74.12 ± 4.74	49.57 ± 4.01	63.25 ± 4.13	15.23 ± 3.24	4.69 ± 3.77

https://doi.org/10.1021/acsomega.3c00605
ACS Omega 2023, 8, 17788−17799

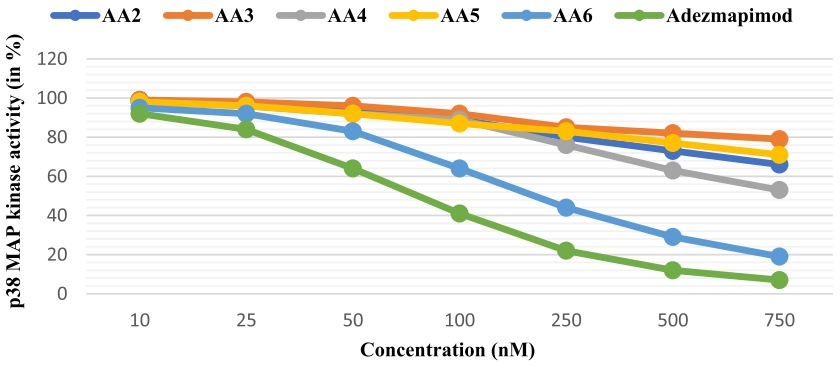

Figure 6. p38 MAP kinase activity (in percent, %) of selected compounds.

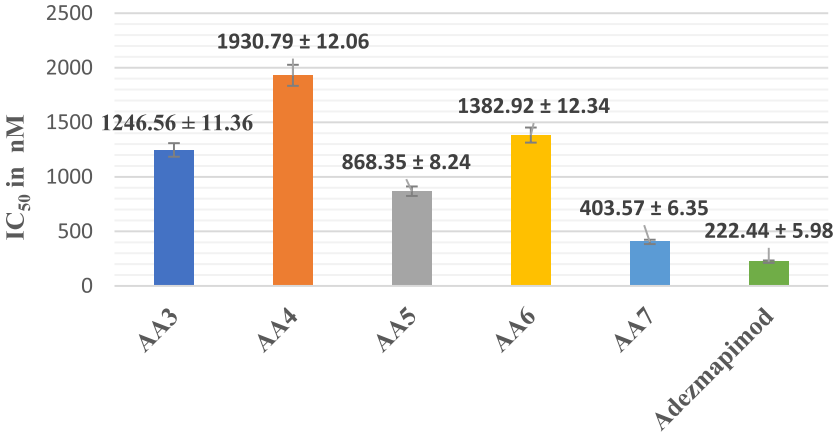

Figure 7. IC_{50} of selected compounds as a function of p38 kinase inhibitory activity.

Table 3. Docking Score of Synthesized Compounds and Adezmapimod

molecules	dock score (kcal/mol)	amino acid is involved in the interaction
AA1	−6.89	Asp 168, Lys 53, Ser 154, and Phe 169
AA2	−7.26	Asp 168, Lys 53, and Met109
AA3	−7.46	Asp 168 and Lys 53
AA4	−7.60	Asp 168, Lys 53, and Tyr 35
AA5	−6.44	Asp 168, Lys 53, and Tyr 35
AA6	−7.83	Asp 168, Lys 53, Tyr 35, Arg 67, and Arg 173
AA7	−7.47	Lys 53, Phe 169, Arg 67, Met109, and Glu 71
AA8	−7.55	Asp 168, Lys 53, and Tyr 35
adezmapimod (SB203580)	−8.02	Lys53, Met109, Ser 154, Glu 71, Tyr 35, Val 38, and Ala 51

prototype p38α MAP kinase inhibitor SB203580. Based on Lipinski's rule of five and Ergan's egg graph, ADME experiments showed that all synthesized compounds were orally active drugs. The compounds also demonstrated good gastrointestinal absorption within the permissible range.

Our study concludes that compound AA6 can be a promising compound if further scaffolds with different substitutions are synthesized for the development of more potent p38α MAP kinase inhibitors.

4. EXPERIMENTAL SECTION

4.1. Materials and Methods. All the chemicals used in the synthesis were supplied by E. Merck, Sigma-Aldrich, Avra, and SD Fine Chemicals. ^{1}H NMR and ^{13}C NMR analyses were carried out on a Bruker Avance 500 spectrometer using tetramethylsilane as an internal standard and DMSO-d_6 as a solvent. Infrared spectra were recorded on a Perkin Elmer FTIR spectrophotometer using KBr and mass spectra were obtained on an Agilant UHD-6450 mass spectrometer. Melting points were recorded in open glass capillaries and are uncorrected. Thin-layer chromatography was performed on pre-coated silica gel plates and column chromatography was performed using silica gel 60−120 mesh.

4.2. Synthetic Procedure. The synthetic route of target compounds (AA1−AA8) is outlined in Figure 2.

4.2.1. Synthesis of [4-(Trifluoromethyl)-1H-imidazole-1-yl] Acetic Acid (4). A solution of the 4-(trifluoromethyl)-1*H*-imidazole (**1**) (0.07 mol, 9.52 g) was mixed in DMF and treated with K_2CO_3 (0.14 mol, 19.55 g) and ethyl bromoacetate (**2**) (0.07 mol, 13.01 g). The reaction mixture was stirred for 18 h at 100 °C and ceased by adding a saturated NH_4Cl (20 mL). The reaction mixture was extracted thrice with 150 mL of ethyl acetate. The organic extracts were combined, dried over anhydrous Na_2SO_4, filtered, and evaporated under reduced pressure to form crude methyl [4-(trifluoromethyl)-1*H*-imidazole-1-yl] acetate (**3**) which was purified by column chromatography with the yield of 85%. Crude product **3** was dissolved in methanol (1.0 mL) and water (0.3 mL) at room temperature and then sodium hydroxide (0.01 mole, 3.87 g) was added. The stirring was done overnight at room temperature. The pH was adjusted between 5 and 6 by the addition of aqueous HCl and the solution was concentrated to half. Solid observed were filtered to yield 80% of [4-(trifluoromethyl)-1*H*-imidazole-1-yl] acetic acid.

https://doi.org/10.1021/acsomega.3c00605
ACS Omega 2023, 8, 17788−17799

Figure 8. Docking pose and molecular interactions of SB203580 in the active site of p38 MAP kinase.

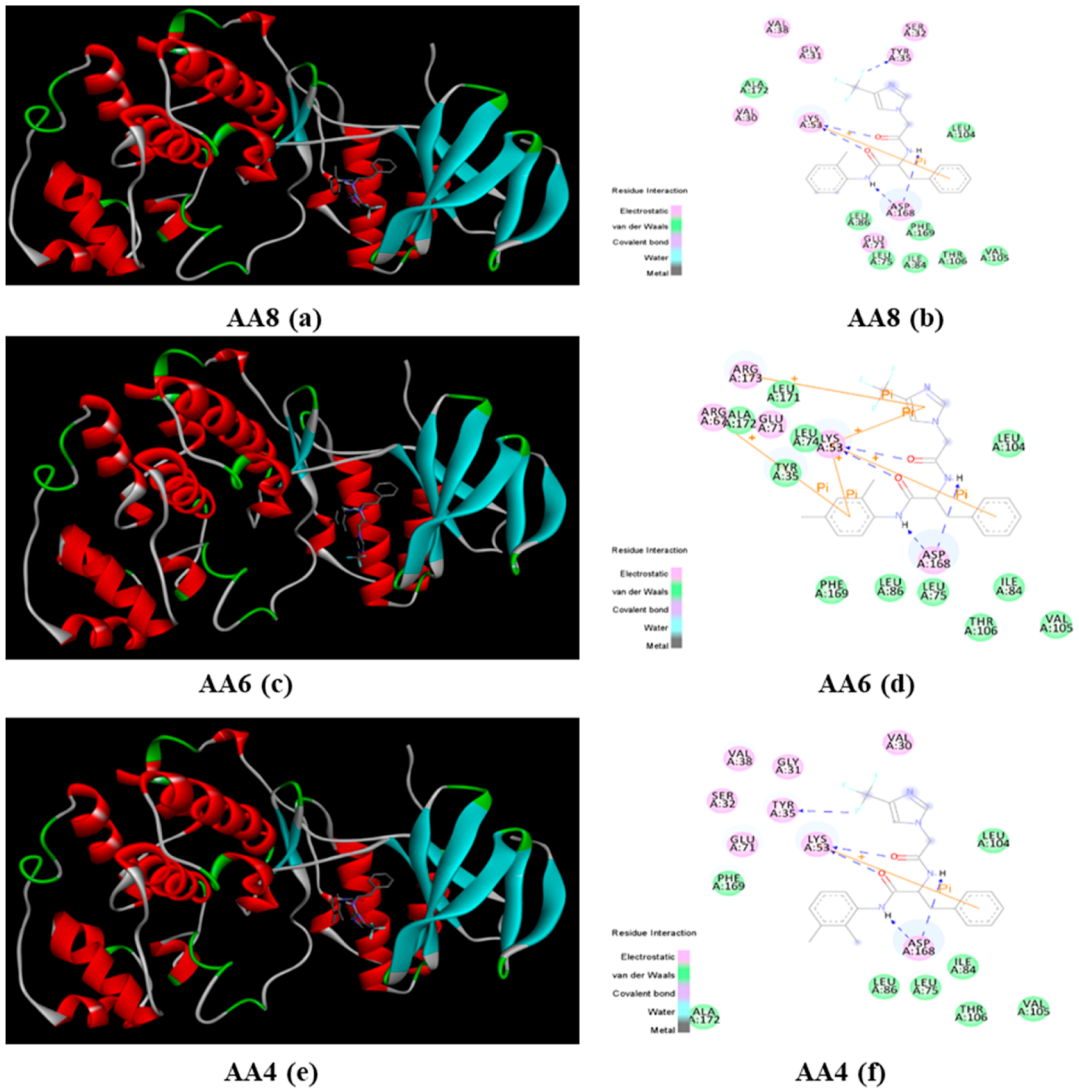

Figure 9. (a,c,e) Docking poses of the compounds **AA8**, **AA6**, and **AA4** in the active site of p38 MAP kinase and (b,d,f) are the molecular interactions of the compounds AA8, AA6, and AA4 in the active site of p38 MAP kinase.

*4.2.2. General Procedure for the Synthesis of 2-Amino-N-(substituted)-3-phenylpropanamide Derivatives (**KO-A1-D to KO-A8-D**).* To a solution of commercially available 2-[(*tert*-butoxycarbonyl) amino]-3-phenylpropanoic acid (**5**) (0.011 mol, 3 g) in DMF (20 mL), HATU (0.015 mol, 5.9 g) was added. To this solution, DIPEA (0.022 mol, 2.92 g) and varying quantity of amine derivatives (A2 to A10) (0.011 mol) ranging from 0.9 g to 1.8 g was added. The resulting mixture was stirred at room temperature for 24 h. Upon completion, water was added and the reaction mixture was extracted thrice with 50 mL of ethyl acetate. The organic layer was separated and washed with brine, dried over anhydrous Na_2SO_4, and

https://doi.org/10.1021/acsomega.3c00605
ACS Omega 2023, 8, 17788−17799

Table 4. Physicochemical Properties of *N*-Substituted [4-(trifluoromethyl)-1*H*-imidazole-1-yl] Amide Derivatives[a]

compound	MW	Lipinski	log *P*	log *S*	HBA	HBD	RB	MR	fraction Csp3
AA1	489.45	0	2.23	−4.45	8	3	12	118.82	0.22
AA2	448.41	0	3.71	−5.03	7	2	10	109.16	0.23
AA3	444.45	0	3.65	−5.37	6	2	11	114.01	0.26
AA4	444.45	0	3.67	−5.3	6	2	10	114.17	0.26
AA5	408.42	0	2.9	−4.24	6	2	10	100.13	0.45
AA6	444.45	0	3.69	−5.3	6	2	10	114.17	0.26
AA7	446.42	0	3.04	−4.7	7	2	11	110.73	0.23
AA18	430.42	0	3.43	−4.92	6	2	10	109.2	0.23
SB203580	377.43	0	3.87	−4.51	4	1	4	105.06	0.05

[a]MW: molecular weight, log *P*: lipophilicity, log *S*: solubility, HBA: number of hydrogen bond acceptors, HBD: number of hydrogen bond donors, RB: rotatable bonds, and MR: molar refractivity.

Table 5. Pharmacokinetic Properties of *N*-Substituted [4-(trifluoromethyl)-1*H*-imidazole-1-yl] Amide Derivatives[a]

compound	TPSA	GIA	BBB P	Pgp S
AA1	128.34	high	no	yes
AA2	76.02	high	no	no
AA3	76.02	high	no	no
AA4	76.02	high	no	no
AA5	76.02	high	yes	yes
AA6	76.02	high	no	no
AA7	85.25	high	no	no
AA8	76.02	high	no	no
SB203580	77.85	high	no	yes

[a]TPSA: topological polar surface area, GIA: gastrointestinal absorption, BBB P: blood brain barrier permeation, and Pgp S: Pgp substrate.

concentrated to dryness and purified using column chromatography to yield the desired compounds, i.e., [2-((*tert*-butoxycarbonyl) amino)-*N*-(substituted)]-3-phenylpropanamide derivatives with the yield of 85% (**KO-A1 to KO-A8**).

The compounds KO-A2 to KO-A10 were taken to a 25 mL reaction flask, dissolved in DMF (10 mL) and stirred in an ice bath. Trifluoroacetic acid (0.005 mol, 0.57g) was added dropwise and then moved to room temperature for 3 h. Completion of the reaction was confirmed by TLC. The solvent was evaporated by rotary evaporation, and the product 2-amino-*N*-(substituted)-3-phenyl propanamide derivatives (**KO-A1-D to KO-A8-D**) was obtained and the residue was purified via column chromatography to afford a compound with the yield of 90%.[18]

*4.2.3. General Procedure for the Synthesis of Target Compounds, i.e., N-Substituted [4-(trifluoro methyl)-1H-imidazole-1-yl] Amide Derivative (**AA1**−**AA8**).* [4-(Trifluoromethyl)-1*H*-imidazole-1-yl] acetic acid (4) (0.0012 mol, 0.25 g) and HATU (0.0012 mol, 0.46 g) were dissolved in DMF (80 mL) to which sodium carbonate (0.0025 mol, 0.27 g) and varying quantity of 2-amino-*N*-(substituted)-3-phenylpropanamide derivatives (KO-A1-D to KO-A8-D) (0.0015 moles) ranging from 0.27 to 0.36 g was added. The reaction mixture was stirred for 24 h at room temperature. Water (100 mL) was added after the completion of the reaction and the reaction mixture was extracted with ethyl acetate (3 × 30 mL). The organic layer was separated and washed with aqueous NaOH, HCl, and brine, dried over anhydrous Na_2SO_4, and concentrated to yield the crude product (**AA1** to **AA8**). The

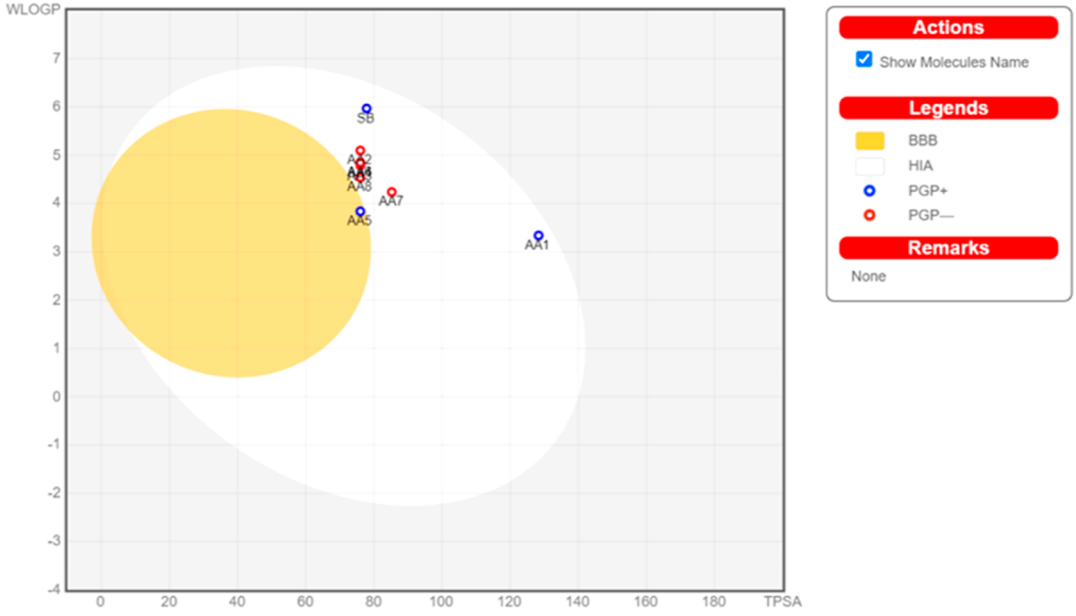

Figure 10. BOILED-Egg approach to predict gastrointestinal absorption and brain penetration of *N*-substituted [4-(trifluoro methyl)-1*H*-imidazole-1-yl] amide derivatives.

https://doi.org/10.1021/acsomega.3c00605
ACS Omega 2023, 8, 17788−17799

crude product was purified by column chromatography and confirmed by ^{1}H NMR and ^{13}C NMR, FTIR, and mass spectroscopy.

*4.2.3.1. 4-Methoxy-3-(3-phenyl-2-(2-(4-(trifluoromethyl)-1H-imidazole-1-yl)acetamido) Propanamido) Benzamide (**AA1**).* The title compound (**AA1**) was synthesized according to the general procedure using 0.365 g of 3-(2-amino-3-phenylpropanamido)-4-methoxybenzamide (KO-A1-D).

White powder, yield: 78%, mp: 343.3 °C. IR (KBr): ν (cm^{-1}) 3291 (N−H_{str}), 1647 (C═O), 1576 (C═N Imidazole), 1118 (C−O). ^{1}H NMR (500 MHz, DMSO-d_6): δ (ppm): 9.51 (s, 1*H*, Amide-*H*), 8.76 (d, *J* = 8.3 Hz, 1*H*, Ar−*H*), 8.34 (s, 1H, Amide-*H*), 7.83 (s, 1H, Imidazole−*H*), 7.66 (m, 2H, Ar−*H*), 7.56 (s, 1H, Imidazole−*H*), 7.32 (d, *J* = 7.1 Hz, 2H, Ar−*H*), 7.27 (t, *J* = 7.5 Hz, 2H, Amide-*H*), 7.22−7.16 (m, 2H, Ar−*H*), 7.07 (d, *J* = 8.6 Hz, 1H, Ar−*H*), 4.88 (d, *J* = 4.4 Hz, 1H, −CH− between two amides), 4.74 (q, *J* = 16.3 Hz, 2H, −CH_2− attached to imidazole), 3.85 (s, 3H, −OCH_3), 3.12 (dd, *J* = 13.5, 4.4 Hz, 1H of −CH**H**− attached to benzene), 2.87 (dd, *J* = 13.4, 9.8 Hz, 1H of −C**H**H− attached to benzene). ^{13}C NMR (500 MHz, DMSO-d_6): δ (ppm): 170.34 (Amide-C), 167.93 (Amide-C), 166.68 (Amide-C), 153.00 (Ar−C), 140.29 (Imidazole−C), 137.89 (Imidazole−CH), 129.81 (Ar−C), 129.09 (Ar−CH), 128.55 (Ar−CH), 128.12 (Ar−CH), 126.87 (Ar−C), 126.70 (Ar−C), 124.98 (Ar−CH), 123.18 (Ar−C), 121.93 (CF_3), 112.77 (Imidazole−CH), 110.91 (Ar−CH), 56.46 (Aliphatic-C, −CH− between two amides), 55.08 (−OCH_3), 49.22 (Aliphatic-C, −CH_2− attached to benzene), 38.26 (Aliphatic-C, −CH_2− attached to Imidazole). ESI-MS (*m*/*z*): 490.16 $[M + H]^+$.

*4.2.3.2. N-(3-Fluoro-4-methylphenyl)-3-Phenyl-2-(2-(4-(trifluoromethyl)-1H-imidazole-1-yl) Acetamido) Propenamide (**AA2**).* Compound **AA2** was synthesized from a general procedure using 0.315 g of 2-amino-*N*-(4-fluoro-3-methyl phenyl)-3-phenylpropanamide (**KO-A2-D**).

Cream color powder, yield: 82%. mp: 342.5 °C, IR (KBr): ν (cm^{-1}) 3291 (N−H_{str}), 1651 (C═O), 1543 (C═N Imidazole), 1412 (C−H). ^{1}H NMR (500 MHz, DMSO-d_6): δ (ppm) 10.28 (s, 1*H*, Ar−*H*), 8.81 (d, *J* = 8.1 Hz, 1*H*, Ar−*H*), 7.69 (s, 1*H*, Amide-*H*), 7.59 (s, 1*H*, Amide-*H*), 7.49 (m, 1*H*, Ar−*H*), 7.27 (s, 1H, Imidazole−*H*), 7.25 (m, 3*H*), 7.20 (dd, *J* = 5.5, 2.9 Hz, 1*H*, Ar−*H*), 7.18 (s, 1*H*, Imidazole−*H*), 7.15 (dd, *J* = 8.2, 1.9 Hz, 1*H*, Ar−*H*), 4.76 (q, *J* = 16.4 Hz, 2*H*, −CH_2− attached to Imidazole), 4.67 (dt, *J* = 14.0, 7.2 Hz, 1*H*, −CH− between two amides), 3.05 (dd, *J* = 13.7, 5.5 Hz, 1*H* of CH**H** attached to benzene), 2.87 (dd, *J* = 13.7, 9.1 Hz, 1H of C**H**H attached to benzene), 2.16 (s, 3*H*, −CH_3). ^{13}C NMR (500 MHz, DMSO-d_6): δ (ppm): 170.18 (Amide-C), 166.61 (Amide-C), 161.61 (Ar−C), 159.69 (Ar−C), 140.33 (Imidazole−C), 138.45 (Ar−C), 138.36 (Ar−CH), 137.62 (Imidazole−CH), 131.94 (Ar−CH), 131.89 (Ar−CH), 129.68 (Ar−CH), 128.64 (Ar−CH), 128.52 (Ar−CH), 126.99 (Ar−CH), 121.96 (CF3), 119.24 (Imidazole−CH), 115.43 (Ar−C), 106.65 (Ar−CH), 55.44 (Aliphatic-C, −CH− between two amides), 49.19 (Aliphatic-C, −CH_2− attached to benzene), 38.45 (Aliphatic-C, −CH_2− attached to Imidazole), 14.12 (−CH_3). ESI-MS (*m*/*z*): 449.15$[M + H]^+$.

*4.2.3.3. N-(3-Ethylphenyl)-3-phenyl-2-(2-(4-(trifluoromethyl)-1H-imidazole-1-yl)acetamido) Propenamide (**AA3**).* Compound **AA3** was obtained according to the described general procedure using 0.310 g of 2-amino-*N*-(3-ethylphenyl)-3-phenylpropanamide (**KO-A3-D**).

Cream color powder, yield: 88%, mp: 340.3 °C. IR (KBr): ν (cm^{-1}) 3276 (N−H_{str}), 1647 (C═O), 1535 (C═N Imidazole), 2922, 3026 (C−H_{str} Aliphatic). ^{1}H NMR (500 MHz, DMSO-d_6): δ (ppm): 10.11 (s, 1H, Amide-*H*), 8.77 (d, *J* = 8.2 Hz, 1H, Ar−*H*), 7.69 (s, 1*H*, Amide-H), 7.59 (s, 1*H*, Imidazole−*H*), 7.40−7.38 (m, 2*H*, Ar−*H*), 7.27 (d, *J* = 4.4 Hz, 4*H*, Ar−*H*), 7.20 (dd, *J* = 8.1, 3.2 Hz, 1*H*, Ar−*H*), 7.18 (s, 1*H*, Imidazole−*H*), 6.90 (d, *J* = 7.7 Hz, 1*H*, Ar−*H*), 4.76 (q, *J* = 16.4 Hz, 2*H*, −CH_2− attached to Imidazole), 4.69 (m, 1*H*, −CH− between two amides), 3.07 (dd, *J* = 13.7, 5.3 Hz, 1*H* of −CH**H**− attached to benzene), 2.87 (m, 1*H* of −C**H**H− attached to benzene), 2.56 (q, *J* = 7.6 Hz, 2*H*, −C**H**$_2$CH$_3$), 1.15 (t, *J* = 7.6 Hz, 3*H*, −CH$_2$C**H**$_3$). ^{13}C NMR (500 MHz, DMSO-d_6): δ (ppm): 169.98 (Amide-C), 166.56 (Amide-C), 144.74 (Ar−C), 140.32 (Imidazole−C), 139.12 (Ar−C), 137.78 (Imidazole−CH), 129.70 (Ar−C), 129.11 (Ar−CH), 128.62 (Ar−CH), 126.94 (Ar−CH), 123.56 (Ar−CH), 121.97 (CF3), 121.94 (Ar−CH), 119.25 (Imidazole−CH), 117.38 (Ar−CH), 117.29 (Ar−CH), 55.45 (Aliphatic-C, −CH− between two amides), 49.22 (Aliphatic-C, −CH_2− attached to benzene), 38.49 (Aliphatic-C, −CH_2− attached to Imidazole), 28.69 (−**C**H$_2$CH$_3$), 15.95 (−CH$_2$**C**H$_3$). ESI-MS (*m*/*z*): 445.18 $[M + H]^+$.

*4.2.3.4. N-(2,3-Dimethylphenyl)-3-phenyl-2-(2-(4-(trifluoromethyl)-1H-imidazole-1-yl)acetamido) Propenamide (**AA4**).* Compound **AA4** was synthesized from a general procedure using 0.310 g of 2-amino-*N*-(2,3-dimethylphenyl)-3-phenylpropanamide (**KO-A4-D**).

Purple color powder, yield: 80%, mp: 351.9 °C, IR (KBr): ν (cm^{-1}) 3272 (N−H_{str}), 1647 (C═O), 1446 (C═N Imidazole), 2922 (C−H_{str} Aliphatic). ^{1}H NMR (500 MHz, DMSO-d_6): δ (ppm): 9.58 (s, 1*H*, Amide-*H*), 8.77 (d, *J* = 8.2 Hz, 1*H*, Ar−*H*), 7.70 (s, 1*H*, Amide-*H*), 7.59 (s, 1*H*, Imidazole−*H*), 7.29 (d, *J* = 4.4 Hz, 4*H*, Ar−*H*), 7.22 (dd, *J* = 8.8, 4.5 Hz, 1*H*, Ar−*H*), 7.02 (m, 2*H*, Ar−*H*), 7.01 (s, 1*H*, Imidazole−*H*), 4.80 (d, *J* = 16.4 Hz, 1*H*, −CH− between two amides), 4.75 (t, *J* = 9.8 Hz, 2*H*, −CH2− attached to imidazole), 3.11 (dd, *J* = 13.5, 5.8 Hz, 1*H* of −CH**H**− attached to benzene), 2.96−2.87 (m, 1*H* of −C**H**H− attached to benzene), 2.21 (s, 3*H*, −CH_3, attached to benzene), 1.93 (s, 3*H*, −CH_3, attached to benzene). ^{13}C NMR (500 MHz, DMSO-d_6): δ (ppm): 170.02 (Amide-C), 166.57 (Amide-C), 140.31 (Ar−C), 137.83 (Imidazole−C), 137.44 (Ar−C), 135.99 (Imidazole−CH), 131.98 (Ar−C), 129.78 (Ar−C), 128.64 (Ar−C), 127.66 (Ar−C), 126.94 (Ar−C), 125.61 (Ar−C), 124.20 (Ar−C), 123.95 (Ar−C), 121.94 (CF_3), 121.91 (Imidazole−CH), 55.04 (Aliphatic-C, −CH− between two amides), 49.32 (Aliphatic-C, −CH_2− attached to benzene), 38.60 (Aliphatic-C, −CH_2− attached to Imidazole), 20.56 (−CH_3− attached to benzene), 14.30 (−CH_3− attached to benzene). ESI-MS (*m*/*z*): 445.18$[M + H]^+$.

*4.2.3.5. N-Cyclopentyl-3-phenyl-2-(2-(4-(trifluoromethyl)-1H-imidazole-1-yl)acetamido) Propenamide (**AA5**).* The titled compound **AA5** was synthesized according to the general procedure from 0.270 g of 2-amino-*N*-cyclopentyl-3-phenylpropanamide (**KO-A5-D**).

White color powder, yield: 88%, mp: 365.9 °C, IR (KBr): ν (cm^{-1}) 3280 (N−H_{str}), 1640 (C═O), 1669 (C═N Imidazole), 2870, 2952 (C−H_{str} Aliphatic). ^{1}H NMR (500 MHz, DMSO-d_6): δ (ppm): 8.63 (s, 1*H*, Amide-*H*), 8.03 (d, *J* = 7.1 Hz, 1*H*, Ar−*H*), 7.68 (s, 1*H*, Amide-*H*), 7.57 (s, 1*H*, Imidazole−*H*), 7.25 (s, 1*H*, Imidazole−*H*), 7.23 (d, *J* = 7.3 Hz, 1*H*, Ar−*H*), 7.18 (dd, *J* = 13.8, 6.9 Hz, 3*H*, Ar−*H*), 4.73 (q, *J* =

https://doi.org/10.1021/acsomega.3c00605
ACS Omega 2023, 8, 17788−17799

16.3 Hz, 2*H*, −CH_2− attached to imidazole), 4.48 (dd, *J* = 14.5, 8.4 Hz, 1*H*, −CH− between two amides), 3.94 (dt, *J* = 13.5, 6.8 Hz, 1*H* of cyclopentyl ring), 2.91 (m, 1*H* of −CH**H**− attached to benzene), 2.77 (dd, *J* = 13.4, 8.6 Hz, 1*H* of −C**H**H− attached to benzene), 1.78−1.62 (m, 2*H* of cyclopentyl ring), 1.62−1.47 (m, 2*H* of cyclopentyl ring), 1.47−1.32 (m, 3*H* of cyclopentyl ring), 1.32−1.16 (m, 1*H* of cyclopentyl ring). ^{13}C NMR (500 MHz, DMSO-d_6): δ (ppm): 170.26 (Amide-C), 166.20 (Amide-C), 162.81 (Ar−C), 140.25 (Ar−CH), 137.96 (Imidazole−C), 129.73 (Imidazole−CH), 128.46 (Ar−CH), 126.75 (Ar−CH), 121.87 (CF_3), 121.84 (Imidazole−CH), 54.73 (Aliphatic-C, −CH− between two amides), 50.71 (−C of cyclopentyl ring), 49.35 (Aliphatic-C, −CH_2− attached to benzene), 38.87 (Aliphatic-C, −CH_2− attached to Imidazole), 32.66 (−CH of cyclopentyl ring), 32.36 (−CH of cyclopentyl ring), 23.88 (−CH of cyclopentyl ring), 23.82 (−CH of cyclopentyl ring). ESI-MS (*m*/*z*): 409 $[M + H]^+$.

*4.2.3.6. N-(2,4-Dimethylphenyl)-3-phenyl-2-(2-(4-(trifluoromethyl)-1H-imidazole-1-yl)acetamido) Propenamide (**AA6**).* Compound **AA6** was obtained according to the described general procedure using 0.311 g of 2-amino-*N*-(2,4-dimethyl phenyl)-3-phenylpropanamide (**KO-A6-D**).

Cream color flake, yield: 92%, mp: 356.4 °C, IR (KBr): ν (cm^{-1}) 3272 (N−H_{str}), 1647 (C═O), 1559 (C═N Imidazole), 2922 (C−H_{str} Aliphatic). ^{1}H NMR (500 MHz, DMSO-d_6): δ (ppm): 9.45 (s, 1*H*, Amide-*H*), 8.76 (d, J = 8.2 Hz, 1*H*, Ar−*H*), 7.70 (s, 1*H*, Amide-*H*), 7.59 (s, 1*H*, Imidazole−*H*), 7.28 (d, *J* = 4.7 Hz, 4*H*, Ar−*H*), 7.23−7.19 (m, 1*H*, Ar−*H*), 7.11 (d, *J* = 8.0 Hz, 1*H*, Ar−*H*), 6.99 (s, 1*H*, Imidazole−*H*), 6.94 (d, *J* = 8.1 Hz, 1*H*, Ar−*H*), 4.79 (d, *J* = 16.3 Hz, 1*H*, −CH between two amides), 4.74 (m, 2*H*, −CH_2− attached to imidazole), 3.10 (dd, *J* = 13.6, 5.8 Hz, 1*H* of −CH**H**− attached to benzene), 2.90 (m, 1*H* of −C**H**H− attached to benzene), 2.23 (s, 3*H*, CH_3 attached to benzene), 2.00 (s, 3*H*, CH_3 attached to benzene). ^{13}C NMR (500 MHz, DMSO-d_6): δ (ppm): 169.91 (Amide-C), 166.55 (Amide-C), 140.31 (Ar−C), 137.83 (Imidazole−C), 135.11 (Ar−C), 133.58 (Imidazole−CH), 132.61 (Ar−C), 131.26 (Ar−CH), 129.77 (Ar−CH), 128.63 (Ar−CH), 126.93 (Ar−CH), 126.88 (Ar−CH), 125.82 (Ar−CH), 125.74 (Ar−CH), 121.93 (Imidazole−CH), 121.90 (CF_3), 55.00 (Aliphatic-C, −CH− between two amides), 49.31 (Aliphatic-C, −CH_2− attached to benzene), 38.66 (Aliphatic-C, −CH_2− attached to Imidazole), 20.94 (CH_3 attached to benzene), 18.01 (CH_3 attached to benzene). ESI-MS (*m*/*z*): 446.18 $[M + H]^+$.

*4.2.3.7. N-(2-Methoxyphenyl)-3-phenyl-2-(2-(4-(trifluoromethyl)-1H-imidazole-1-yl)acetamido) Propenamide (**AA7**).* Compound **AA7** was obtained according to the described general procedure using 0.313 g of 2-amino-*N*-(2-methoxyphenyl)-3-phenylpropanamide (**KO-A7-D**).

Cream color powder, yield: 95%, mp: 341.7 °C, IR (KBr): ν (cm^{-1}) 3265 (N−H_{str}), 1647 (C═O), 1539 (C═N Imidazole), 2937 (C−H_{str} Aliphatic), 1114 (C−O). ^{1}H NMR (500 MHz, DMSO-d_6): δ (ppm): 9.40 (s, 1*H*, Amide-*H*), 8.74 (d, *J* = 8.3 Hz, 1*H*, Ar−*H*), 7.87 (dd, *J* = 7.9, 1.4 Hz, 1*H*, Ar−*H*), 7.68 (s, 1*H*, Amide-*H*), 7.56 (s, 1*H*, imidazole−*H*), 7.30 (t, *J* = 7.8 Hz, 3*H*, Ar−*H*), 7.26 (d, *J* = 7.7 Hz, 1*H*, Ar−*H*), 7.19 (t, *J* = 7.1 Hz, 1*H*, Ar−*H*), 7.08 (m, 1*H*, Ar−*H*), 7.03 (dd, *J* = 8.2, 1.3 Hz, 1*H*, Ar−*H*), 6.90 (s, 1*H*, imidazole−*H*), 4.89 (td, *J* = 9.0, 4.9 Hz, 1*H*, −CH− between two amides), 4.74 (q, *J* = 16.3 Hz, 2*H*, −CH_2− attached to imidazole), 3.80 (s, 3*H*, O−CH_3), 3.11 (dd, *J* = 13.7, 4.8 Hz, 1*H* of −CH**H**− attached to benzene), 2.87 (dd, *J* = 13.7, 9.6 Hz, 1*H* of −C**H**H− attached to benzene). ^{13}C NMR (500 MHz, DMSO-d_6): δ (ppm): 170.18 (Amide-C), 166.66 (Amide-C), 150.34 (Ar−C), 140.29 (Ar−C), 137.88 (Imidazole−C), 129.83 (Imidazole−CH), 128.54 (Ar−CH), 127.22 (Ar−CH), 126.86 (Ar−CH), 125.28 (Ar−CH), 122.61 (Ar−CH), 121.91 (CF_3), 121.88 (Ar−CH), 121.50 (Ar−CH), 120.70 (Ar−CH), 111.75 (Imidazole−CH), 56.16 (OCH_3), 55.09 (Aliphatic-C, −CH− between two amides), 49.24 (Aliphatic-C, attached to benzene), 38.26 (Aliphatic-C, attached to Imidazole). ESI-MS (*m*/*z*): 447.16 $[M + H]^+$.

*4.2.3.8. N-(2,5-Dimethylphenyl)-3-phenyl-2-(2-(4-(trifluoromethyl)-1H-imidazole-1-yl)acetamido) Propenamide (**AA8**).* Compound **AA8** was obtained according to the described general procedure using 0.311 g of 2-amino-*N*-(2,5-dimethyl phenyl)-3-phenyl propanamide (**KO-A8-D**).

White powder, yield: 80%, mp: 353.6 °C, IR (KBr): ν (cm^{-1}) 3272 (N−H_{str}), 1647 (C═O), 1535 (C═N Imidazole), 3026, 2922 (C−H_{str} Aliphatic). ^{1}H NMR (500 MHz, DMSO-d_6): δ (ppm): 9.52 (s, 1*H*, Amide-*H*), 8.78 (d, *J* = 8.2 Hz, 1*H*, Ar−*H*), 7.94 (s, 1*H*, Imidazole−*H*), 7.71 (s, 1*H*, Amide-*H*), 7.60 (d, *J* = 1.1 Hz, 1*H*, Ar−*H*), 7.29 (d, *J* = 4.3 Hz, 4*H*, Ar−*H*), 7.25 (s, 1*H*. imidazole−*H*), 7.22 (dd, *J* = 8.9, 4.4 Hz, 1*H*, Ar−*H*), 7.18 (d, *J* = 7.6 Hz, 1*H*, Ar−*H*), 7.15 (t, *J* = 7.5 Hz, 1*H*, Ar−*H*), 7.08 (m, 1*H*, Ar−*H*), 4.79 (d, *J* = 9.3 Hz, 1*H*, −CH− between two amides), 4.76 (dd, *J* = 12.8, 9.5 Hz, 2*H* of −CH_2 attached to imidazole), 3.11 (dd, *J* = 13.6, 5.8 Hz, 1*H* of −CH**H**− attached to benzene), 2.92 (dd, *J* = 13.5, 8.9 Hz, 1*H* of −C**H**H− attached to benzene), 2.05 (s, 3*H*, −CH_3 attached to benzene). ^{13}C NMR (500MHz, DMSO-d_6): δ (ppm): 170.01 (Amide-C), 166.64 (Amide-C), 162.85 (Ar−C), 140.30, 137.79 (Imidazole−C), 136.16 (Ar−C), 132.74 (Imidazole−C), 130.75 (Ar−C), 129.76 (Ar−CH), 128.64 (Ar−CH), 126.95 (Ar−CH), 126.37 (Ar−CH), 126.04 (Ar−CH), 125.83 (Ar−CH), 121.91 (CF_3), 121.87 (Imidazole−C), 55.16 (Aliphatic-C, between two amides), 49.31 (Aliphatic-C, attached to benzene), 38.52 (Aliphatic-C, attached to Imidazole), 18.04 (CH_3 attached to benzene). ESI-MS (*m*/*z*): 445.18 $[M + H]^+$.

4.3. In Vitro Anti-Inflammatory Activity. *4.3.1. Evaluation of Albumin Denaturation Inhibitory Activity of Synthesized Compounds.* The denaturation of proteins is one of the most well-known causes of inflammation. As part of the investigation, eight test samples AA1−AA8 were evaluated for their anti-inflammatory properties. The protein denaturation assay was performed.[19] Various concentrations of test samples were prepared at 100, 200, and 300 μg/mL, and each reaction mixture was prepared by mixing with 0.5 mL of 1.5 mg/mL bovine serum albumin (BSA) and incubating at 37 °C for 20 min. The reaction mixtures were then heated for 3 min at 57 °C. Phosphate buffer (0.5 M, pH 6.3) with a volume of 250 μL was added to each mixture, which was thoroughly mixed. Then, after equal distribution of molecules in each reaction mixture, 100 μL of each mixture was transferred into separate test tubes, and Folin−Ciocalteu's reagent was added in the same proportion by volume. After 10 min of incubation at 55 °C, the tubes were allowed to cool, and absorbance was determined at the wavelength of 650 nm using a Multimode Microplate Reader (Tecan Sunrise, USA). Diclofenac sodium (100 μg/mL) was used to evaluate the recorded measurements as a reference drug. The inhibition percentage of protein denaturation was calculated using the following formula

https://doi.org/10.1021/acsomega.3c00605
ACS Omega 2023, 8, 17788−17799

%denaturation inhibition

$$= [Abs_{control} - (Abs_{test}/Abs_{control})] \times 100$$

4.3.2. Evaluation of In Vitro p38 MAP Kinase Inhibitory Assay for the Synthesized Compounds. In the present study, a nonradioactive immunosorbent assay for p38 kinase activity has been used, which can be used routinely for the screening of small-molecule inhibitors of p38 kinase. An ATF-2 substrate was used for phosphorylation, which showed linearity between 5-30 ng/well. Based on this analysis, 15 ng/well at a 1.5 h incubation period was determined to be optimal. The p38 kinase substrate ATF-2 (10 μg/mL in TBS) was coated onto microtiter plates for 1.5 h at 37 °C. The remaining open binding sites were blocked with blocking buffer (BB; 0.05% Tween 20, 0.25% BSA, 0.02% NaN_3 in TBS) for 30 min at room temperature, following three washings with distilled water. The plates were then washed again, and the plates were incubated at 37 °C for 1 h. Test solutions such as AA2, AA3, AA4, AA5, and AA6 containing 15 ng/well p38 MAPK were diluted in kinase buffer (50 mM Tris, pH 7.5, 10 mM $MgCl_2$, 10 mM β-glycerophosphate, 100 μg/mL BSA, 1mM dithiothreitol, 0.1 mM Na_3VO_4, and 100 μg/mL rATP), with or without test substance (ranging from 0.01 to 1.0 μM). After the subsequent washing, plates were blocked with BB for 15 min and washed four times. Wells were filled with 50 μL of the specific anti-bis-($Thr^{69/71}$)-phospho-ATF-2 (AB, 1:500 in BB) and incubated for 1 h at 37 °C followed by washing and consecutive incubation with 50 μL of the secondary antibody [AB (alkaline phosphatase-conjugated), 1:1400 in BB]. Then, 100 μL of 4-NPP was pipetted in each well after a final washing step, and color development was measured 1.5−2 h later with an enzyme-linked immunosorbent assay reader at 405 nm (Tecan, Sunrise, USA). Percent enzyme activity and IC_{50} were calculated based on the kinase measurement values using megalin software 4.21.

4.4. Molecular Docking of *N*-Substituted [4-(trifluoromethyl)-1*H*-imidazole-1-yl] Amide Derivative. Molecular docking studies were done in AutoDock 4.2. The docking study was performed in order to investigate the binding ability of the novel *N*-substituted [4-(trifluoromethyl)-1*H*-imidazole-1-yl] amide derivative to the binding site of the p38α MAP kinase protein. The docking scores were found out.

4.4.1. Protein Preparation. The protein 3D crystal structure of p38α MAP kinase (PDB: 1A9U, resolution: 2.50 Å) was retrieved in PDB format from the Protein Data Bank (PDB), and the 3D protein structure was refined and energy minimized before docking analysis. Missing atoms, polar hydrogens, and Kollman charges were added to refine the protein, whereas crystallographic water molecules, foreign ligands, and unnecessary ions were deleted. The docking procedure involved the employment of a flexible ligand and a rigid protein.

4.4.2. Ligand Preparation. The 3D structure of the proposed ligands was drawn using ACD Lab Chemsketch and saved in mol 2 molecular format. These mol 2 structures were converted into pdbqt format using MGL tools 1.5.7.

4.4.3. Docking. Docking studies were performed with AutoDock 4.2 using the Lamarckian genetic algorithm. The flexible docking procedure was used for a p38α MAP kinase protein and a flexible ligand. A grid of 60, 60, and 60 points was created in the x, y, and z directions. A grid spacing of 0.375 Å using Autogrid Grid 4 and a distance-dependent function of the dielectric constant were used for the calculation of the energy map. The default settings were used for all other parameters. At the end of docking, the ligand with the most favorable free energy of binding was noted. Each molecule was docked using AutoDock 4.2 with parameters ga_num_evals and ga_run set to 25 000 000 and 50, respectively, as suggested. Molecular interaction diagrams are obtained from DS 4.0 visualizer. The entire calculations were carried out on PC-based machines running Linux as an operating system.[20]

4.5. ADME Studies. The ADME (absorption, distribution, metabolism, and excretion) properties of compounds were assessed using Swiss ADME software. According to Lipinski's rule of five, compounds observed good oral bioavailability if the compound's molecular weight is < 500. All compounds followed the rule. The gastrointestinal safety profile was also performed using Swiss ADME software. The list of SMILES was uploaded on these online web servers, and the required attributes of the desired compounds were created.[21]

■ ASSOCIATED CONTENT

Supporting Information

The Supporting Information is available free of charge at https://pubs.acs.org/doi/10.1021/acsomega.3c00605.

FTIR, ^{1}H NMR, ^{13}C NMR, and MS spectra of the final compounds; ^{1}H NMR of intermediate compounds; and docking structures of the final compounds (PDF)

■ AUTHOR INFORMATION

Corresponding Author

Md Azizur Rahman − *Department of Pharmaceutical Chemistry, Faculty of Pharmacy, Integral University, Lucknow, Uttar Pradesh 226026, India;* orcid.org/0000-0002-3069-8329; Email: marahman@iul.ac.in

Authors

Archana Awasthi − *Department of Pharmaceutical Chemistry, Sri Venkateshwara College of Pharmacy, Hyderabad 500081 Telangana, India; Department of Pharmaceutical Chemistry, Faculty of Pharmacy, Integral University, Lucknow, Uttar Pradesh 226026, India*

Mantripragada Bhagavan Raju − *Department of Pharmaceutical Chemistry, Sri Venkateshwara College of Pharmacy, Hyderabad 500081 Telangana, India*

Complete contact information is available at: https://pubs.acs.org/10.1021/acsomega.3c00605

Notes

The authors declare no competing financial interest.

■ ACKNOWLEDGMENTS

Authors are thankful to Sri Venkateshwara College of Pharmacy, Surabhi Educational Society, Hyderabad and the Faculty of Pharmacy, Integral University, Lucknow for its research atmosphere, motivation to do research work, and providing necessary facilities to do the work (Manuscript Communication Number: IU/R&D/2023-MCN0001909).

■ REFERENCES

(1) Yang, G.; Chang, C. C.; Yang, Y.; Yuan, L.; Xu, L.; Ho, C. T.; Li, S. Resveratrol Alleviates Rheumatoid Arthritis via Reducing ROS and Inflammation, Inhibiting MAPK Signaling Pathways, and Suppressing Angiogenesis. *J. Agric. Food Chem.* **2018**, *66*, 12953−12960.

(2) Long, Y.; Zhao, Y.; Ma, X.; Zeng, Y.; Hu, T.; Wu, W.; Deng, C.; Hu, J.; Shen, Y. Endoplasmic reticulum stress contributed to inflammatory bowel disease by activating p38 MAPK pathway. *Eur. J. Histochem.* **2022**, *66*, 3415.
(3) Romero-Becerra, R.; Santamans, A. M.; Folgueira, C.; Sabio, G. p38 MAPK Pathway in the Heart: New Insights in Health and Disease. *Int. J. Mol. Sci.* **2020**, *21*, 7412.
(4) Falcicchia, C.; Tozzi, F.; Arancio, O.; Watterson, D. M.; Origlia, N. Involvement of p38 MAPK in Synaptic Function and Dysfunction. *Int. J. Mol. Sci.* **2020**, *21*, 5624.
(5) Raghavendra, N. M.; Pingili, D.; Kadasi, S.; Mettu, A.; Prasad, S. V. U. M. Dual or multi-targeting inhibitors: The next generation anticancer agents. *Eur. J. Med. Chem.* **2018**, *143*, 1277−1300.
(6) Grimes, J. M.; Grimes, K. V. p38 MAPK inhibition: A promising therapeutic approach for COVID-19. *J. Mol. Cell. Cardiol.* **2020**, *144*, 63−65.
(7) Yeung, Y. T.; Aziz, F.; Guerrero-Castilla, A.; Arguelles, S. Signaling Pathways in Inflammation and Anti-inflammatory Therapies. *Curr. Pharm. Des.* **2018**, *24*, 1449−1484.
(8) Chen, L.; Deng, H.; Cui, H.; Fang, J.; Zuo, Z.; Deng, J.; Li, Y.; Wang, X.; Zhao, L. Inflammatory responses and inflammation-associated diseases in organs. *Oncotarget* **2017**, *9*, 7204−7218.
(9) Cuadrado, A.; Nebreda, A. R. Mechanisms and functions of p38 MAPK signalling. *Biochem. J.* **2010**, *429*, 403−417.
(10) Sabio, G.; Davis, R. J. TNF and MAP kinase signalling pathways. *Semin. Immunol.* **2014**, *26*, 237−245.
(11) Yang, C.; Cao, P.; Gao, Y.; Wu, M.; Lin, Y.; Tian, Y.; Yuan, W. Differential expression of p38 MAPK α, β, γ, δ isoforms in nucleus pulposus modulates macrophage polarization in intervertebral disc degeneration. *Sci. Rep.* **2016**, *6*, 22182.
(12) Awasthi, A.; Raju, M. B.; Rahman, M. A. Current Insights of Inhibitors of p38 Mitogen-Activated Protein Kinase in Inflammation. *Med. Chem.* **2021**, *17*, 555−575.
(13) Kong, T. T.; Zhang, C. M.; Liu, Z. P. Recent Developments of p38α MAP Kinase Inhibitors as Antiinflammatory Agents Based on the Imidazole Scaffolds. *Curr. Med. Chem.* **2013**, *20*, 1997−2016.
(14) Kulkarni, R. G.; Laufer, S. A.; Chandrashekar, V. M.; Garlapati, A. Synthesis, p38 kinase inhibitory and anti-inflammatory activity of new substituted benzimidazole derivatives. *Med. Chem.* **2013**, *9*, 91−99.
(15) Dunetz, J. R.; Magano, J.; Weisenburger, G. A.; Gerald, A. W. Large-Scale Applications of Amide Coupling Reagents for the Synthesis of Pharmaceuticals. *Org. Process Res. Dev.* **2016**, *20*, 140−177.
(16) Sabatini, M. T.; Boulton, L. T.; Sneddon, H. F.; Sheppard, T. D. A green chemistry perspective on catalytic amide bond formation. *Nat. Catal.* **2019**, *2*, 10−17.
(17) Wilson, K. L.; Murray, J.; Jamieson, C.; Watson, A. J. B. Cyrene as a bio-based solvent for HATU mediated amide coupling. *Org. Biomol. Chem.* **2018**, *16*, 2851−2854.
(18) Wang, L.; Casey, M. C.; Vernekar, S. K. V.; Sahani, R. L.; Kankanala, J.; Kirby, K. A.; Du, H.; Hachiya, A.; Zhang, H.; Tedbury, P. R.; Xie, J.; Sarafianos, S. G.; Wang, Z. Novel HIV-1 capsid-targeting small molecules of the PF74 binding site. *Eur. J. Med. Chem.* **2020**, *204*, 112626.
(19) Williams, L. A. D.; O'connar, A.; Latore, L.; Dennis, O.; Ringer, S.; Whittaker, J. A.; Conrad, J.; Vogler, B.; Rosner, H.; Kraus, W. The in vitro anti-denaturation effects induced by natural products and non-steroidal compounds in heat-treated (immunogenic) bovine serum albumin is proposed as a screening assay for the detection of anti-inflammatory compounds, without the use of animals, in the early stages of the drug discovery process. *West Indian Med. J.* **2008**, *57*, 327.
(20) Dhanik, A.; McMurray, J. S.; Kavraki, L. E. DINC: A new AutoDock-based protocol for docking large ligands. *BMC Struct. Biol.* **2013**, *13*, S11.
(21) Daina, A.; Michielin, O.; Zoete, V. SwissADME: a free web tool to evaluate pharmacokinetics, drug-likeness and medicinal chemistry friendliness of small molecules. *Sci. Rep.* **2017**, *7*, 42717.

https://doi.org/10.1021/acsomega.3c00605
ACS Omega 2023, 8, 17788−17799